
APST

Asia-Pacific Journal of Science and Technology
<https://www.tci-thaijo.org/index.php/APST/index>

 Published by Research and Innovation Department,
 Khon Kaen University, Thailand

Investigation and machine learning prediction of one-way progressive pump abrasive flow machining prototype: SKD61 (AISI H13) hot work steel

 Theerapong Maneepen¹ and Parinya Srisattayakul^{2,*}
¹Program in Engineering and Technology Management, Faculty of Engineering, Rajamangala University of Technology Krungthep, 10120 Thailand,

²Department of Industrial Engineering, Faculty of Engineering, Rajamangala University of Technology Krungthep, 10120 Thailand

 *Corresponding author: parinya.sr@mail.rmutk.ac.th

Received 21 June 2024

Revised 1 July 2024

 Accepted 20 November 2024

Abstract

The objectives are to study the effects of tooling pressure and machining time on surface roughness regulatory affairs (Ra) of hot work steel SKD 61 involving an abrasive flow machining (AFM) polishing prototype and to compare the design of experiments (DOE), factorial regression, and predictive machine learning (ML). The research steps include defining the objectives, identifying the important factors and their levels, designing the experiments, conducting experiments and collecting data, and analyzing the results statistically. The ML process was performed with a program, the experimental results were compared and concluded. A progressive pump (NETZSCH) was used to conduct the experiments on the AFM curved samples. Experiments were conducted to investigate machined, hardened, polished samples with abrasive papers from #180 to #1200 and were measured with the initial Ra values against the final value. The process parameters were pressure 1, 2, and 3 bar; sample hardness SKD61; 45±2 HRC; abrasive particle size (Al₂O₃) 5.0 microns (μm) (concentration 50% by weight, silicone oil). The results showed that 3 bar and 20 min, pressure, and cycle time consequently gave the best results. The average Ra of the workpieces was 0.057 to 0.042 microns, and the delta between surface roughness (SR) was 0.006 to 0.012 μm. The comparison of experimental and prediction results using RapidMiner ML showed only minor differences, indicating better precision control for industrial applications.

Keywords: Abrasive Flow Machining, Surface Roughness, Design of Experiment, Machine Learning

1. Introduction

Abrasive media can flow through a workpiece's internal passages, achieving high-resolution finishing with increased accuracy and faster polishing. This article examines the effect of tool clearance on surface roughness (SR) of hot work steel (SKD61), comparing experimental design (DOE), factorial regression, and machine learning (ML) predictions. A prototype machine was developed using a rotating rotor pump to push abrasive paste over a workpiece surface. This novel technique uses viscoelastic abrasive media to polish surfaces and remove burrs from complex internal geometry to enhance fluid flow properties and optimize component functionality. An initial review of articles about abrasive flow machining (AFM) found that there were research studies on the following: 1) the mechanical basis of AFM, 2) mathematical simulation, 3) assistance of magnetic fields, 4) using the rotation of the workpieces together, 5) studying abrasives with various substances and 6) using ultrasonic assistance.

AFM development is shown in the schematic [1]. Frictional wear from the slow flow of particle suspensions is caused by the dispersive particle phase, compared to the finite element method (FEM) prediction [2]. A theoretical analysis is proposed that can be estimated and compared with experimental data from the literature [3]. The study investigates AFM process parameters such as cycle number, abrasive, size, concentration, etc. on material removal rate (MR) and SR. It aims to identify dominant parameters influencing concentration, mesh size,

surface roughness, cycles, material removal rate, surface finish improvement (ΔRa), and flow rate on aluminum and brass workpieces. These were analyzed using a scanning electron microscope (SEM) and compared to theoretical models. Lathe setup experiments with turret steady rests focused on minimum material removal rate (MRR) (oscillation speed and orbital amplitude) within a speed range of 400 to 1200 RPM [4]. The surface simulation was created in the process, and the parametric analysis was performed using an artificial neural network (ANN) with 4 inputs, 2 outputs, and 1 hidden layer to model the process. A second network was run in parallel with ALM: augmented Lagrange multiplier algorithm [5]. Experimental studies were performed to understand AFM with MAAFM: magnetically assisted AFM [6], [7]. The study examined the burr in spring collets (chrome-molybdenum) that occurs within small and large diameters [8]. It also investigated Al alloy, Al alloy/SiC, and Al alloy/SiC 0%, 10%, and 15%; consequently, metal matrix composites (MMCs) (R-AFF: Rotational-AFF) (significant effect) ΔRa [9], [10]. computational fluid dynamics (CFD) numerical method was used in designing a suitable approach to find the SR on the complex shape of the hole (passageway) [11], [12], [13], [14].

The study used AISI D2 (American Iron and Steel Institute; Cool work tool steel), electrical discharge machine (EDM) pre-machined hardened tool steel ($\sim 10 \mu m$) [15], [16]. This was similar to previous experiments [17]. Tooling pressure and machining time on the surface and geometry tolerances, AISI4140, increases the corrosive medium viscosity and progresses the abrasive efficiency rounding as measured with the generalized Maxwell model [18], [19]. The essential parameters' effects on finishing EN-8 steel bevel gears have been investigated [20]. From 1.4 to 1.8 μm (initial SR), ultrasonic-assisted Abrasive Flow Finishing (AFF); bevel gears [21]. A model process parameter has been developed for ceramic materials [22]. SLM: selective laser melting is the modern process used for experimentation [23], [24], [25].

In 2020, there was an AFM study, that showed the mathematical equation for the difference in SR and percentage improvement in the surface finish (PISF), which determines the primary parameters: the polishing passes number (20, 40, and 60), the force used (800 Kgf.), the temperature (32 °C), and the volume of the abrasive flowing through the workpiece (200 cm³). Experiments were done with ring-shaped cylindrical aluminum alloy pieces and the max-% improvement SR was noted [26]. AFM studies were performed on internal channels by selective laser melting (SLM) specimens. To find the surface roughness value, x-ray diffraction (XRD) was performed, and SEM photographs were taken of the workpiece sintered into wrought bars [27]. In 2023, three studies were conducted with different workpieces: first, AFF, a copper workpiece made from adaptive moment estimation (ADAM) company (additively manufactured nano-finish) using abrasive visco-elastic hydrogel (Siloxane, natural or synthesized elastomers, thermoplastic polymers), a cost-effective, eco-friendly, and biodegradable. The dependent variables are the surface roughness value and the rate of metal removal [28]. AFF experiments were done with helical gear micro pre-diameters: 4, 6, 8, and 12 mm., 40 mm x width: 40 mm x height: 10 mm length. This was done to determine the improved gear surface quality to improve the gear toothings [29]. AFM experiment on AISI 304 with pre-diameters of 4, 6, 8, and 12 mm. Workpiece: 40 x 40 x 10 mm². Cassava starch medium for internal surface finishing; shear thickening polishing slurry was used: STP-s. Numerical simulation was done using polyborosiloxane mixed with SiC as the polishing agent. Dependent variables were finished surface roughness and metal removal rate, which were photographed with an AFM [30].

The study examines the following parameters; ON, OFF, and SV; surface quality; and machining time in WEDM, multi-ANOVA. Machine learning: ML algorithms like support vector regression (SVR) and polynomial regression were examined. Comparative analysis showed that SVR best predicts the SR (Ra) and machining time, performing and providing more accurate predictions than simpler regression models [31]. Using tree-based ML algorithms known for their simplicity, preciseness, and consistency. Multiple prediction models are constructed and evaluated. An experimental setup measures spring back angles for various manufacturing conditions. The data sets are then randomly divided into 90% training and 10% testing [32]. Investigates various prediction models for spontaneous coal combustion, a feed-forward neural network (FFNN) is a prediction model with two hidden layers: a 2HL network architecture to provide the best performance with a 5-minute prediction capability [33].

ML is used to learn and adapt between the inputs and the outputs quickly. ML algorithms are algorithms with reliable and accurate results. This can be done where data can be sufficient to provide high accuracy for the predicted results for hot work metal. The method includes pressure to a different 3 level. The final SR is measured using a Keyence VR-6000 Series 2D (line profile).

Polishing a surface to high smoothness requires a precise and convenient machine. This study focuses on developing such a machine using a unidirectional abrasive flow concept with aluminum oxide mixed with silicone oil. Inspection sensors like pressure or flow rate will be developed further. Due to high construction costs, a preliminary prototype is needed. The study examines the effect of tool clearance on SR (Ra) SKD61 hot work tool steel with factorial regression to receive the desired surface roughness and compare experimental and machine learning results. Successful research will improve and differentiate the prototype.

2. Materials and methods

2.1 Materials

SKD 61 workpiece, aluminum oxide (Al_2O_3) $0.5\ \mu\text{m}$, silicone oil., hardness of specimens SKD61 45 ± 2 HRC were used for testing. The workpiece is formed by turning it to the specified shape and hardening. Figure 1 shows SKD61: tool steel/mold steel/middle carbon steel, high hardness, wear resistance, hardenability, thermal fatigue, high precision long-life hot work die mold. It is used to produce cutting tools, cold/hot work molds, and measuring tools, as well as pistons, valves, valve seats, diesel engine fuel pump seats, pressing dies, punching machines, and other tools that work under high-temperature conditions.



Figure 1 Workpiece of 1-way progressive pump abrasive flow machining prototype.

2.2 Methods

2.2.1 Prepare the workpiece and abrasive media

For the method, the researchers prepared the SKD 61 workpiece surface with sandpaper from grades #180 to #1200 and then mixed abrasive media Al_2O_3 $0.5\ \mu\text{m}$ 50% concentration by weight in silicone oil.

2.2.2 Design of experiment

The researchers elected two key factors: pressure (p) and cycle time (t). The desired results are shown in Table 1. Set Factor Levels. For instance, choose three levels of pressure (p) 1, 2, and 3 bar, and three levels of machining time (t) 10 minutes, 15 minutes, and 20 minutes. A factorial design systematically combines the two factors' different levels, see Figure 2 for a full factorial design.

Table 1 Controlled parameters for the experiment.

Parameter	Detail
Material	SKD61 Hardness $\pm 45\pm 2$ HRC
Pressure (p) (bar)	1, 2, 3
Cycle time (t) (min)	10, 15, 20
Particle type & size	Al_2O_3 , 0.5 micron
Concentration (% by weight),	50 (Silicon Oil-based)
Initial SR	P180 to P1200

2.2.3 Experimental set-up

The procedure for installing the experimental equipment consisted of a workpiece clamping set that included a lock to keep the workpiece in a specified position. This was to allow the abrasive to flow through the workpiece, which can be adjusted to suit workpieces of different shapes. The pre-experimental installation with the unidirectional grinding machine used the power from the electric motor through the clutch set and the drive shaft of the piggyback to create pressure to drive the abrasive to run along the pipe and flow to grind with the surface of the specimen continuously. There is a pressure gauge installed in the system. The holder was used to hold different characteristics of the specimens. NETZSCH pumps are used in the food industry.

Factor Information						
Factor	Levels Values					
pressure	3 1, 2, 3					
time	3 10, 15, 20					
#	C1	C2	C3	C4	C5	C6
	StdOrder	RunOrder	PtType	Blocks	pressure	time
1	21	1	1	1	1	20
2	19	2	1	1	1	10
3	4	3	1	1	2	10
4	23	4	1	1	2	15
5	9	5	1	1	3	20
6	12	6	1	1	1	20
7	1	7	1	1	1	10
8	5	8	1	1	2	15
9	7	9	1	1	3	10
10	18	10	1	1	3	20
11	6	11	1	1	2	20
12	22	12	1	1	2	10
13	14	13	1	1	2	15
14	17	14	1	1	3	15
15	10	15	1	1	1	10
16	24	16	1	1	2	20
17	25	17	1	1	3	10
18	8	18	1	1	3	15
19	3	19	1	1	1	20
20	2	20	1	1	1	15
21	13	21	1	1	2	10
22	16	22	1	1	3	10
23	26	23	1	1	3	15
24	15	24	1	1	2	20
25	11	25	1	1	1	15
26	27	26	1	1	3	20
27	20	27	1	1	1	15

Figure 2 The experimental plan (DOE: Design of Experiment).

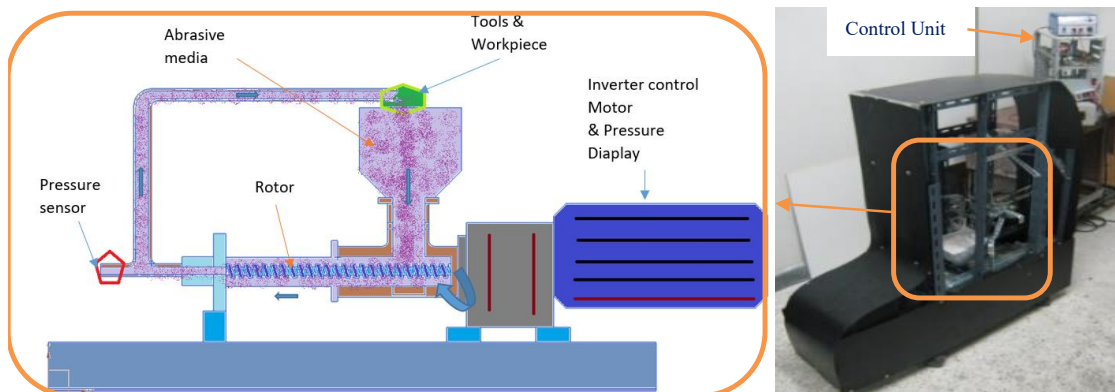


Figure 3 Tools and Equipment of the one-way rotor AFM prototype.

AFM experiments to ensure the corrected conditions were implemented. The study used SR (Ra) microns before the AFM process. Consequently, polishing was done by a rotor AFM prototype within cycle time: 10 minutes, 15 minutes, and 20 minutes. The researchers measured and recorded the responses after the experiment. This could involve quantifying surface roughness or assessing other relevant performance indicators. The surface roughness was measured after being polished by AFM (Final SR) using the 2D profile measurement, Keyence VR-6000 Series 2D (Figure 4). These specific tools were used for their proven accuracy and reliability.



Figure 4 Displaying the surface measurement using Keyence 2D line measurement (non-contact/vision).

2.2.4. Statistical Analysis Method

To analyze data, ANOVA: Analysis of Variance was used to identify significant main effects and interactions that play a crucial role in Abrasive Flow Machining (AFM) data analysis and interpretation. The statistical analyses used were AFM and Regression Analysis. Regression Analysis models the relationship between independent variables (e.g.; process parameters) and dependent variables (e.g.; surface roughness). Experimental Design (DOE): is a statistical approach that systematically determines the optimal process parameters. ANOVA & Regression Analysis to identify significance, optimize, and understand their AFM performance. These statistical analyses provide quantitative insights into the performance, optimization, and control of AFM processes. Minitab 19 was used in order to apply statistical methods in the AFM research of the machining process.

2.2.5 Machine Learning Analysis

The ML process starts with selecting target data, entering the process, transforming the process, and then entering data mining. The results were analyzed to finally gain knowledge. This was done using RapidMiner software version 10, The working of the ML program has steps as shown in Figure 5. This was done in order to interpret the results and draw conclusions in an objective context and report the steps to thoroughly document the experiment (preparation, methods, and results). A comprehensive document summarizing findings was prepared. This was carried out through varying two key factors. Their effects on the AFM process were then examined, namely AFM's optimization and performance characteristics for specific objectives.

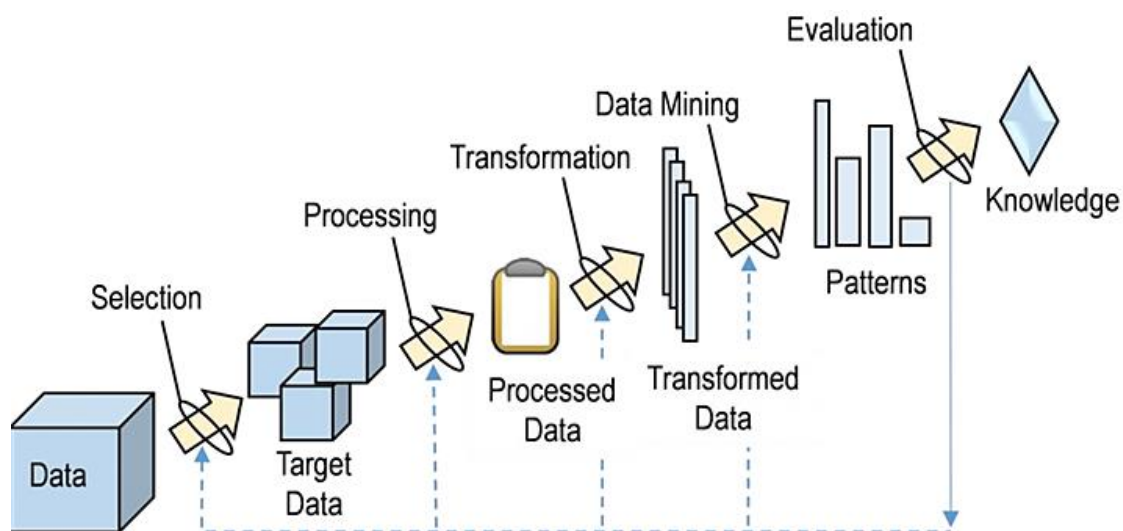


Figure 5 Steps of data mining [34].

3. Results and discussions

3.1 Surface Roughness & Profile Detection

A 2D measurement of the curved surface of SKD61 was performed and the results were summarized and discussed. The surface smoothness results were obtained from the specified pressure and time shown in Table 2. It was found that the surface smoothness values tended to give better values.

Table 2 Displays pressure 1 bar, 2 bar, 3 bar: time 0 minutes to 10 minutes, 15 minutes, and 20 minutes, 3 replicates.

Time	1 bar	2 bar	3 bar
	Δ SR (Ra)	Δ SR (Ra)	Δ SR (Ra)
10	0.006	0.008	0.010
	0.007	0.007	0.006
	0.008	0.008	0.009
15	0.007	0.009	0.011
	0.009	0.010	0.011
	0.009	0.009	0.010
20	0.009	0.011	0.012
	0.010	0.011	0.012
	0.010	0.011	0.011

The following shows the polished workpiece's surface profile and Figure 6 shows the surface roughness in 2D and Ra (micron) with the AFM prototype.

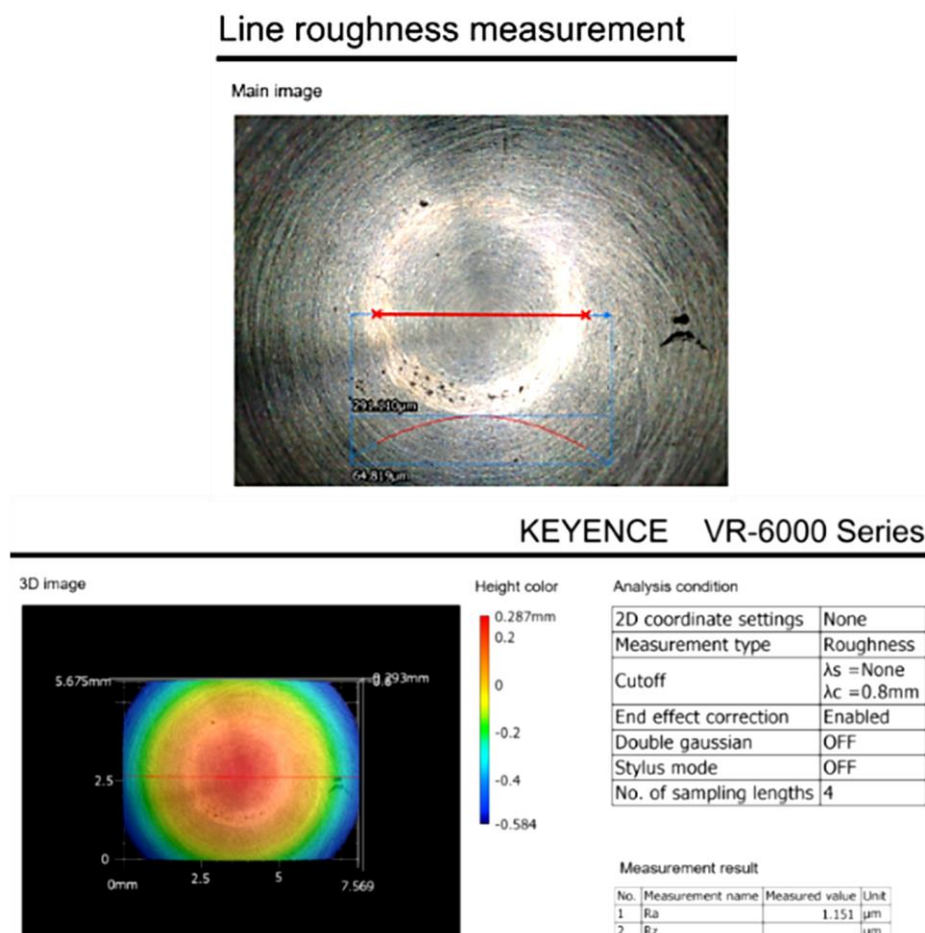


Figure 6 Surface roughness polishing with the rotor AFM prototype.

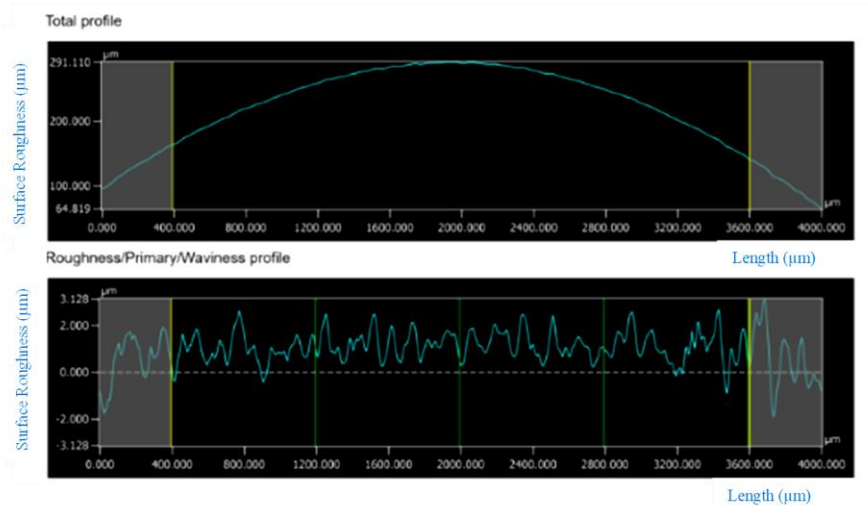


Figure 6 (Cont.) Surface roughness polishing with the rotor AFM prototype.

Table 2 displays SR: Surface Roughness (micron); parameters: 1 bar, 2 bar, and 3 bar; and the time from 0 minutes to 10 minutes, 15 minutes, and 20 minutes. Average surface roughness (SR) before value and after value, there is a tendency to decrease the SR (Ra) from 0.057 to 0.042 microns.

There was a decreasing trend in the surface roughness value (Ra) from 0.057 to 0.044 microns. At 1 bar of pressure, the difference between the before and after values of the average SR (Ra) was Δ 0.006 to 0.010 microns. At a pressure of 2 bar, the difference before and after the average SR (Ra), 0.058 to 0.043 μm , showed a trend to decrease. The difference is Δ 0.007 to 0.011 μm at a pressure of 3 bar; the difference before and after the value of average SR (Ra) was 0.057 to 0.042 μm . The difference was Δ 0.006 to 0.012 μm .

3.2 Statistical Analysis Methods

Analysis was performed to confirm that the experimental results were accurate. This reflects the performance of the developed prototype polishing machine designed and created with the aim of achieving more accurate results.

Figure 7 and Figure 8 illustrate the pressure and time data and linear model results for SR. The obtained regression equation shows the delta SR value in Figure 7. The analysis of the variance table shows that the P-value is less than 0.05, indicating that pressure and time significantly affect the response. The correlation coefficient (R²) can be found in the regression analysis chapter where R-Sq (adj) = 80.74%; less than 70% is considered acceptable. The relationship equation between factor and response is the Pareto graph. Notice that the bar graph of factors A and B is past the critical line, indicating that they all significantly affect the results. The main effect graph shows how the factors of pressure, and time affect SR. A 3 bar pressure factor and a 20-minute time period gave the best effect on surface roughness.

General factorial regression: delta SR versus pressure, time

Factor Information		
Factor	Levels	Values
pressure	3	1, 2, 3
time	3	10, 15, 20

Analysis of Variance					
Source	DF	Adj SS	Adj MS	F-Value	P-Value
Model	8	0.000061	0.000008	14.62	0.000
Linear	4	0.000059	0.000015	28.50	0.000
pressure	2	0.000030	0.000015	28.50	0.000
time	2	0.000030	0.000015	28.50	0.000
2-Way Interactions	4	0.000002	0.000000	0.75	0.571
pressure*time	4	0.000002	0.000000	0.75	0.571
Error	18	0.000009	0.000001		
Total	26	0.000070			

Model Summary				
S	R-sq	R-sq(adj)	R-sq(pred)	
0.0007201	86.67%	80.74%	70.00%	

Coefficients					
Term	Coef	SE Coef	T-Value	P-Value	VIF
Constant	0.009333	0.000139	67.35	0.000	
pressure					
1	-0.001222	0.000196	-6.24	0.000	1.33
2	-0.000111	0.000196	-0.57	0.578	1.33
time					
10	-0.001222	0.000196	-6.24	0.000	1.33
15	-0.000111	0.000196	-0.57	0.578	1.33
pressure*time					
1 10	0.000111	0.000277	0.40	0.693	1.78
1 15	-0.000333	0.000277	-1.20	0.245	1.78
2 10	-0.000333	0.000277	-1.20	0.245	1.78
2 15	0.000222	0.000277	0.80	0.433	1.78

Figure 7 Factor Information and ANOVA: delta SR versus pressure, time, and regression equation for general factorial regression.

Fits and Diagnostics for Unusual Observations

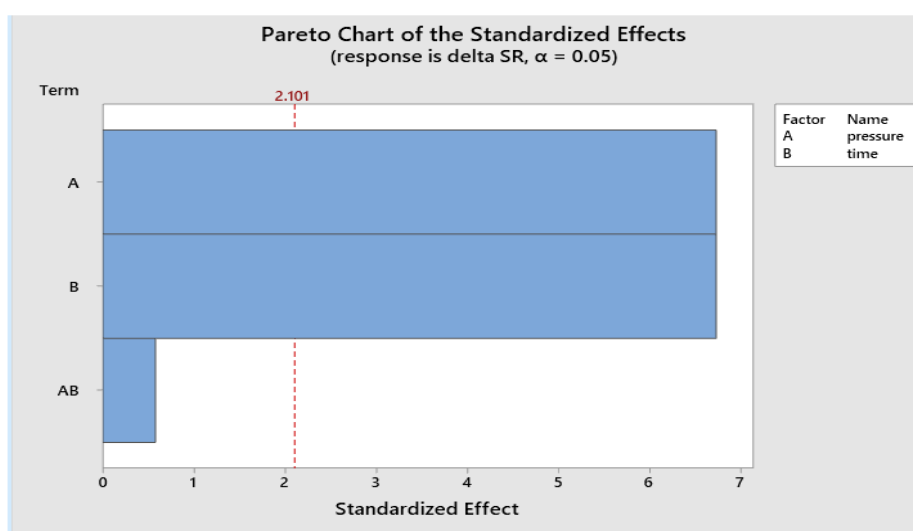
Obs	delta SR	Fit	Resid	Std Resid
5	0.009000	0.007667	0.001333	2.27 R

R Large residual

Regression Equation

```
delta SR = 0.009333 - 0.001222 pressure_1 - 0.000111 pressure_2 + 0.001333 pressure_3
- 0.001222 time_10 - 0.000111 time_15 + 0.001333 time_20
+ 0.000111 pressure*time_1 10 - 0.000333 pressure*time_1 15
+ 0.000222 pressure*time_1 20 - 0.000333 pressure*time_2 10
+ 0.000222 pressure*time_2 15 + 0.000111 pressure*time_2 20
+ 0.000222 pressure*time_3 10 + 0.000111 pressure*time_3 15
- 0.000333 pressure*time_3 20
```

Figure 7 (Cont.) Factor Information and ANOVA: delta SR versus pressure, time, and regression equation for general factorial regression.



Factorial Plots for delta SR

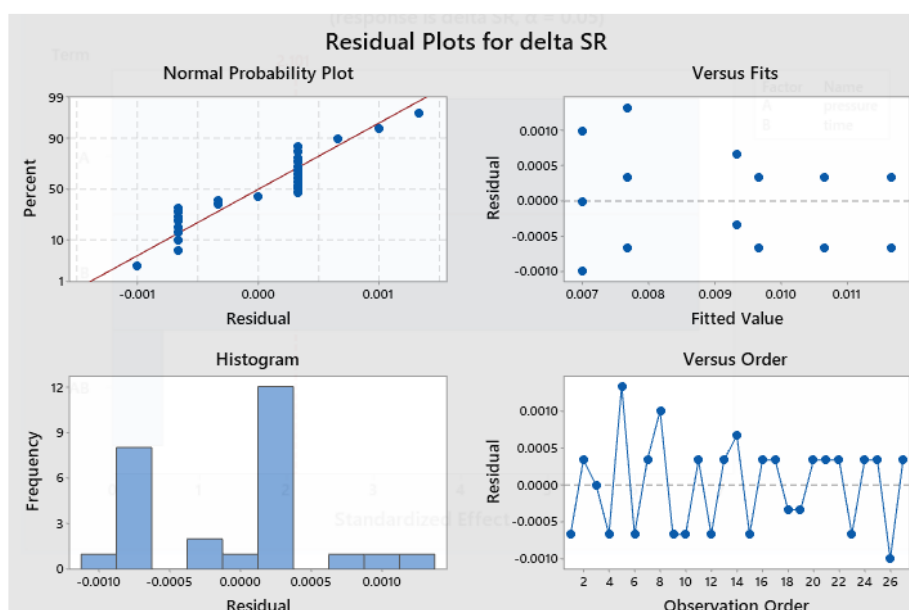


Figure 8 Pareto Chart, Residual Plots, Main Effects Plot, and Interaction Plot for delta SR.

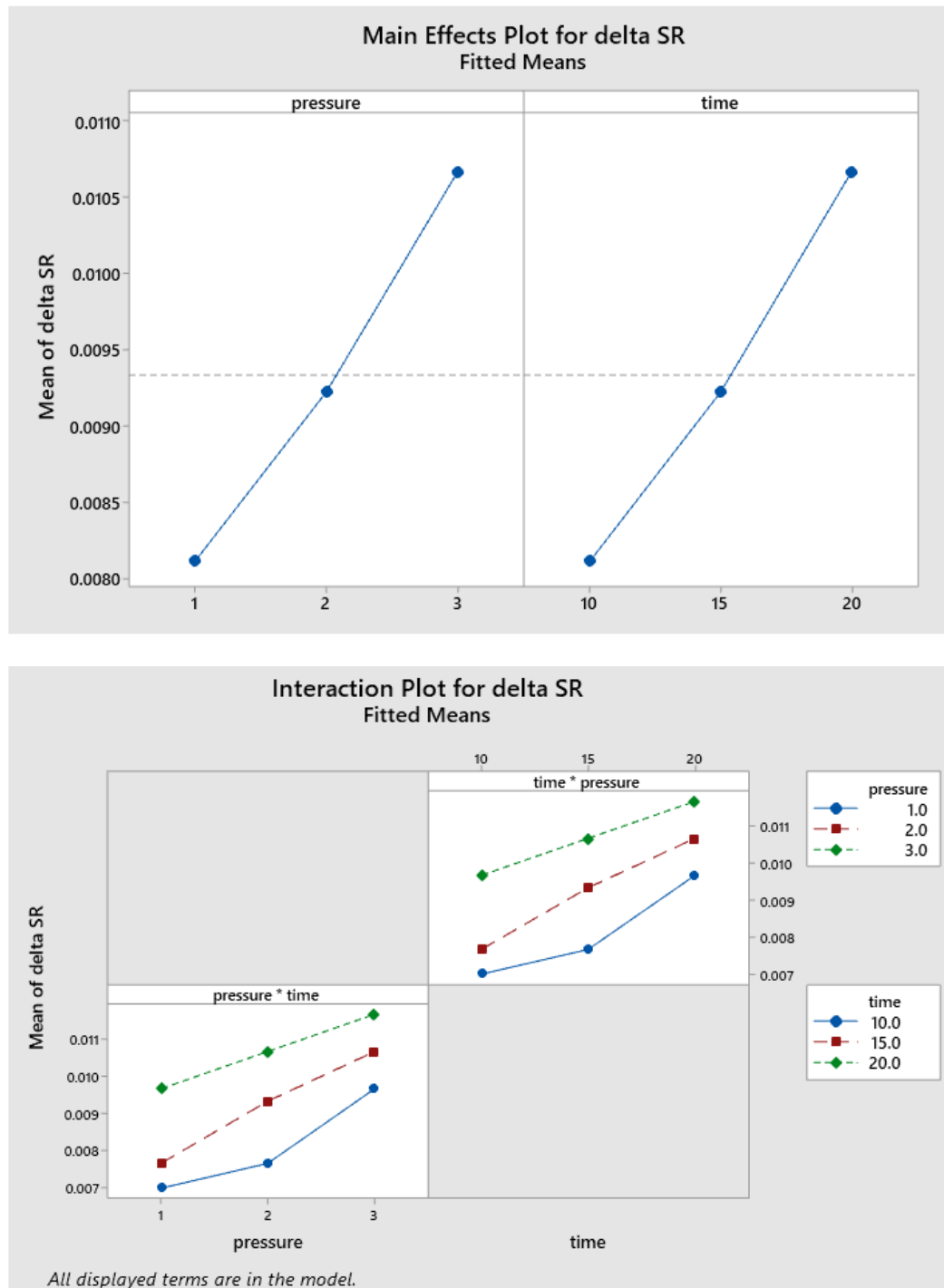


Figure 8 (Cont.) Pareto Chart, Residual Plots, Main Effects Plot, and Interaction Plot for delta SR.

3.3 Machine Learning Prediction

ML predictions with the RapidMiner 10 program were used to make predictions about expected experiment results from actual experimental results in order to compare with the predictions. This is in order to make the selection of various parameters more accurate. The linear regression function was used with a flow chart and selected attributes process, as shown in Figure 9.

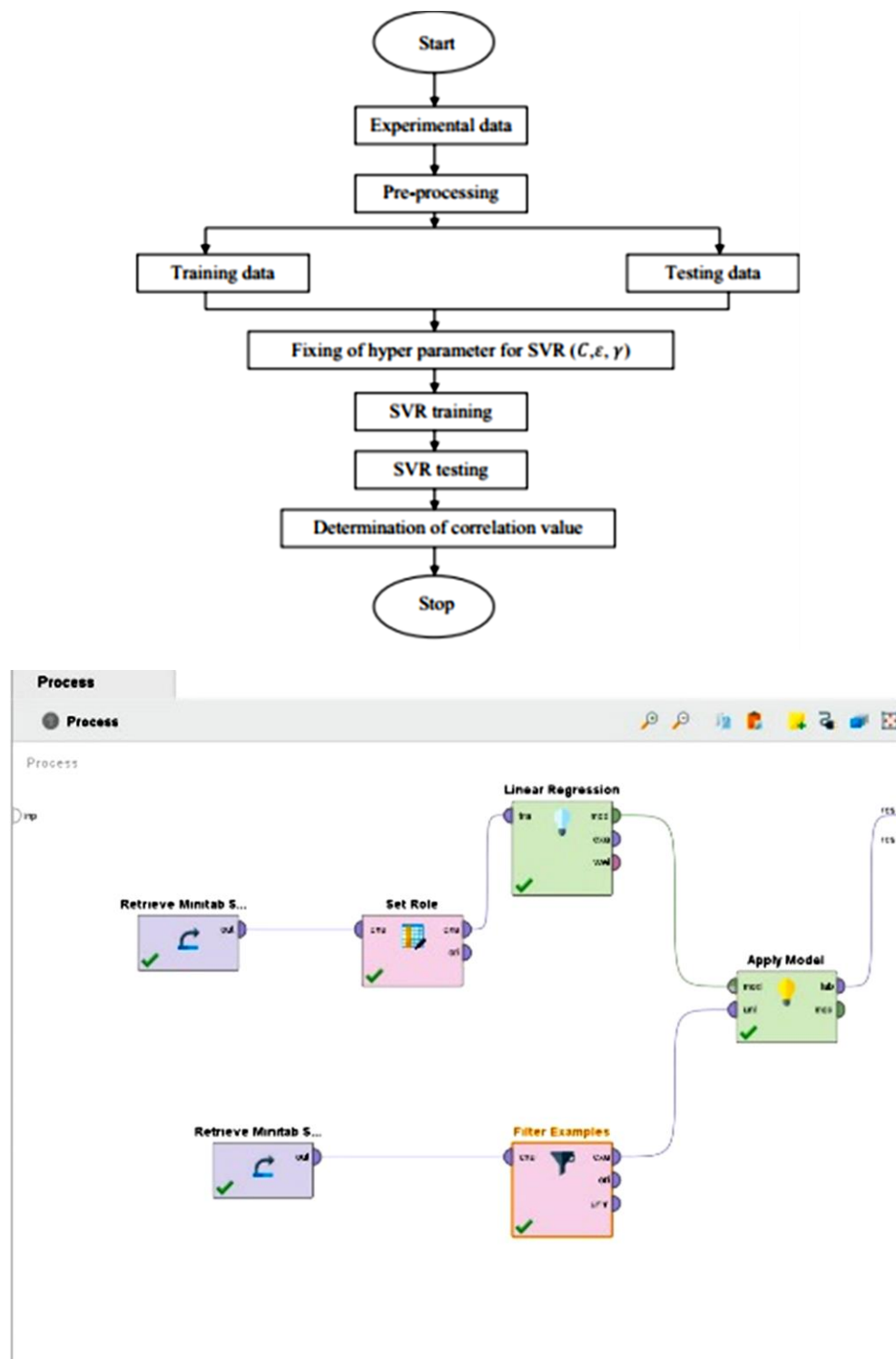


Figure 9 Flow chart of a standard SVR model and select attributes process.

The sub-work steps that turn raw data into knowledge were selection, process, transformation, data lining, and evaluation to achieve target data, then processed data, transformed data, and patterns (Figure 5). Through inputting raw data from Minitab 19, the results show the prediction (delta SR) in Figure 10 and uses the model, parameters (pressure, time, delta SR, and cross-validation), see Figure 11. Performance vector: root means squared error: 0.001 ± 0.001 (micro average: 0.001 ± 0.000).

Open in Turbo Prep Auto Model Interactive Analysis

Open in Turbo Prep Auto Model Interactive Analysis

Row No.	pressure	time	delta SR
1	1	20	0.012
2	1	10	0.008
3	2	10	0.008
4	2	15	0.009
5	3	20	0.013
6	1	20	0.010
7	1	10	0.006
8	2	15	0.009
9	3	10	0.010
10	3	20	0.012
11	2	20	0.011
12	2	10	0.008
13	2	15	0.010
14	3	15	0.011
15	1	10	0.007
16	2	20	0.010
17	3	10	0.009
18	3	15	0.011

Row No.	delta SR	prediction(d...	pressure	time
1	0.012	0.010	1	20
2	0.009	0.009	2	15
3	0.010	0.008	3	10
4	0.013	0.012	3	20
5	0.010	0.009	2	15
6	0.010	0.011	2	20
7	0.011	0.010	3	15
8	0.008	0.010	1	20
9	0.010	0.010	1	20
10	0.009	0.009	3	10
11	0.006	0.009	3	10
12	0.012	0.012	3	20
13	0.010	0.010	3	15
14	0.009	0.008	1	15
15	0.008	0.006	1	10
16	0.006	0.006	1	10
17	0.007	0.008	1	15
18	0.007	0.007	1	10

Figure 10 Input data from Minitab 19 and prediction with ML (delta SR).

Result History
ExampleSet (Apply Model) ✕

Name

Type

Missing

Statistics

Filter (4 / 4 attributes):

Min

Max

Average

✓ Prediction prediction(delta SR)	Real	0	Min 0.007	Max 0.012	Average 0.009
✓ pressure	Integer	0	Min 1	Max 3	Average 2
✓ time	Integer	0	Min 10	Max 20	Average 15
✓ delta SR	Real	0	Min 0.003	Max 0.013	Average 0.009

Attribute	Coefficient	Std. Error	Std. Coefficient	Tolerance	t-Stat	p-Value	Code
pressure	0.001	0.000	0.360	1	2.848	0.009	***
time	0.000	0.000	0.698	1	5.528	0.000	****
(Intercept)	0.002	0.001	?	?	1.465	0.156	

Figure 11 Apply model; pressure, time, delta SR, and cross-validation with Rapid Miner.

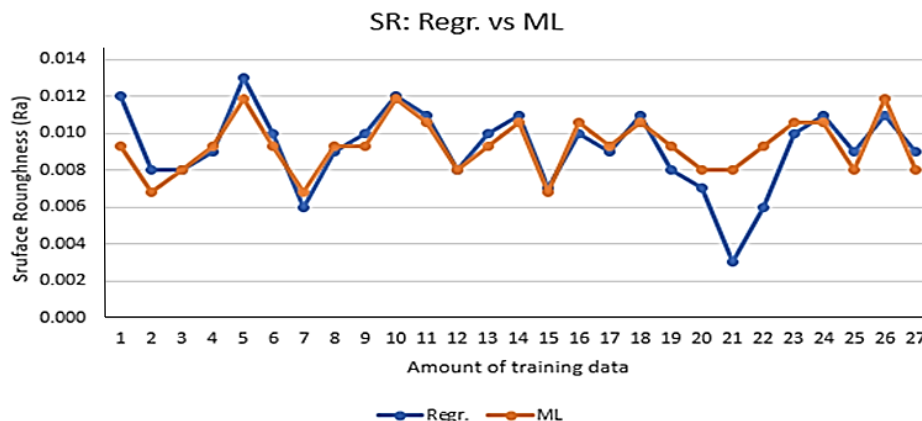


Figure 12 compares the experimental results with the ML predictions that give similar results. The results show the correlation coefficient of pressure and time, minimum value, maximum value, mean value, and P-value statistical value affecting surface roughness.

4. Conclusions

The study examined the development of a prototype machine using a rotary pump to push abrasives along a specified surface. The first objective of this paper was to study the effects of tooling pressure and machining time on the surface roughness/SR (Ra) of SKD61 hot work steels, which showed promising results. Experiments using silicone oil mixed with 50 wt% aluminum oxide (Al₂O₃) revealed significant improvements compared to previous unidirectional methods. SKD61 steel specimens showed reduced roughness (delta 0.006 to 0.012 μm). The results showed that 3 bar pressure and a 20-minute time period gave the best difference, with AFM results confirming the high-quality surface finish. The second objective was to compare the effects of tooling pressure and machining time on the surface roughness (Ra) of SKD61 hot work steels using factorial regression and machine learning. ML predictions using Rapid Miner to improve the accuracy of parameter selection. The results showed only minor differences, indicating better precision control that can be applied for industrial applications. Future developments will integrate AI technology and ESP32 Arduino with sensors such as temperature, ultrasonic, etc. to improve accuracy and control, making this method suitable for complex shapes, micro-mold production, and parts.

5. References

- [1] Nitin Dixit, Varun Sharma, Pradeep Kumar. Research trends in abrasive flow machining: A systematic review. *J Manuf Process*. 2021;64: 1434-1461.
- [2] J.J. Hann, P.S. Steif. Abrasive wear due to the slow flow of a concentrated suspension, *Wear*.1998; 219:177-183.
- [3] Rajendra K. Jain, Vijay K. Jain, P.M. Dixit. Modeling of material removal and surface roughness in the abrasive flow machining process. *Int J Mach Tools Manuf*.1999; 39: 1903-1923.
- [4] V.K. Jain, and S.G. Adsul. Experimental investigations into abrasive flow machining (AFM). *Int J Mach Tools Manuf*. 2000; 49: 1003-1021.
- [5] Jun Wang, William Scott, Liangchi Zhang. Abrasive technology: current development and applications I, World Scientific. Singapore. 1999;2: 269-317.
- [6] Sehijpal Singh, H.S. Shan, P. Kumar. Wear behavior of materials in magnetically assisted abrasive flow machining. *J Materials Process Technol*. 2002;128(1-3):155-161.
- [7] P.D. Kamble, et al. Use of magneto abrasive flow machining to increase material removal rate and surface finish, *Mechanical. Automobile Product Eng*. 2012; 2: 249-262.
- [8] Kim JD, Kim KD. Deburring of burrs in spring collects by abrasive flow machining. *Int J Adva Manuf Technol*. 2004;24: 469-473.
- [9] Sankar MR, et. al. Experimental investigations into rotating workpiece abrasive flow machining. *Wear*. 2009;267: 43-51.
- [10] Jain R.K, Jain V.K, Kalra P.K. Modeling of abrasive flow machining process: a neural network approach. *Wear*. 1999; 231:242-248.
- [11] WANG AC, et al. Uniform surface polished method of complex holes in abrasive flow machining. *Trans Nonferrous Met Soc China*. 2009;19: 250-257.
- [12] Uhlmann E, et al. CFD simulation of the abrasive flow machining process. *Procedia CIRP*. 2015;31: 209-214.

- [13] Kumar S, et al. Nanofinishing of freeform surfaces (knee joint implant) by rotational-magnetorheological abrasive flow finishing (R-MRAFF) process. *Precis Eng.* .2015;42: 165-178.
- [14] Sharma VK, Modeling and analysis of a novel rotational magnetorheological abrasive flow finishing process. *Int J Lightweight Mater Manuf.* 2021;4: 290-301.
- [15] Kenda J, et al. Surface integrity in abrasive flow machining of hardened tool steel AISI D2. *Procedia Eng.* 2011;9: 172-177.
- [16] Bahre D, et al. Investigation of one-way abrasive flow machining and in-process measurement of axial forces. *Procedia CIRP.* 2012; 1:419-424.
- [17] Swat M, et al. Improved process control and model of axial forces of one-way abrasive flow machining. *Procedia CIRP.* 2014; 14:19-24.
- [18] Bremerstein T, et al. Wear of abrasive media and its effect on abrasive flow machining results. *Wear* 2015;1: 44-51.
- [19] Wang AC, et al. A study on the abrasive gels and the application of abrasive flow machining in complex-hole polishing. *Procedia CIRP.* 2018; 68: 523-528.
- [20] Venkatesh G, et al. Finishing of bevel gears using abrasive flow machining, *Procedia Eng.* 2014; 97: 320-328.
- [21] Venkatesh G, et al. On ultrasonic assisted abrasive flow finishing of bevel gears. *J Mach Tools Manuf.* 2015; 89: 29-38.
- [22] Uhlmann E, et al. A pragmatic modeling approach in abrasive flow machining for complex-shaped automotive components. *Procedia CIRP.* 2016; 64: 51-54.
- [23] Chaneac MSD, et al. Characterization of maraging steel 300 internal surface created by selective laser melting (SLM) after abrasive flow machining (AFM). *Procedia CIRP.* 2018; 77: 359-362.
- [24] Han S, et al. Surface integrity in abrasive flow machining (AFM) of internal channels created by selective laser melting (SLM) in different building directions. *Procedia CIRP.* 2020;87: 315-320.
- [25] Dixit N, Sharma V, Kumar P, Experimental investigations into abrasive flow machining (AFM) of 3D printed ABS and PLA parts. *Rapid Prototyp J.* 2022;28(1):161-174.
- [26] Baraiya R, et al. In-situ simultaneous surface finishing using abrasive flow machining via novel fixture. *J Manuf Process.* 2020; 50: 266-278.
- [27] Han S, et al. Surface integrity in abrasive flow machining (AFM) of internal channels created by selective laser melting (SLM) in different building directions. *Procedia CIRP.* 2020; 87: 315-320.
- [28] Basha SM, et al. Development and performance evaluation of galactomannan polymer-based abrasive medium to finish atomic diffusion additively manufactured pure copper using abrasive flow finishing. *Additive Manuf.* 2023; 61: 103-290.
- [29] Ansari IA, et al. Effect of ground tire rubber media's viscoelasticity and flow passage geometry on the abrasive flow finishing of helical gear. *J Manuf Process.* 2023;101: 219-233.
- [30] Dong X, et al. Fine finishing of internal surfaces using cassava starch medium. *J Mater Process Technol.* 2023; 315: 117918.
- [31] Lomozik L, et al. Optimization of WEDM parameters using machine learning: a comparative analysis of selected regression models. *Int J Modern Manufa Technol.* 2023; 15(2): 2067–3604.
- [32] Wasif M, et al. Prediction of spring back using the machine learning technique in high-tensile strength sheet metal during the V-bending process, *Jordan J Mech Ind Eng.* 2023; 17: 481-488.
- [33] Ismail FB, et al. A machine learning approach for fire-fighting detection in the power industry. *Jordan J Mech Ind Eng.* 2021; 15(5): 475-482.
- [34] Rodjanaburanon N. Data analysis manual: Rapid Miner Studio. 2022; 1: 9-45.